Applied Physics Letters

Propulsion kinematics of achiral microswimmers in viscous fluids

Cite as: Appl. Phys. Lett. **118**, 204103 (2021); https://doi.org/10.1063/5.0048277
Submitted: 21 February 2021 . Accepted: 27 April 2021 . Published Online: 21 May 2021

Prateek Benhal, David Quashie, U Kei Cheang, and Jamel Ali

AIP Publishing

Applied Physics Letters ARTICLE scitation.org/journal/apl

Propulsion kinematics of achiral microswimmers in viscous fluids

Cite as: Appl. Phys. Lett. **118**, 204103 (2021); doi: 10.1063/5.0048277
Submitted: 21 February 2021 · Accepted: 27 April 2021 ·
Published Online: 21 May 2021

Prateek Benhal,[1,2,a] David Quashie, Jr.,[1,2,a] U Kei Cheang,[3,a] and Jamel Ali[1,2,b]

AFFILIATIONS

[1]Department of Chemical and Biomedical Engineering, FAMU-FSU College of Engineering, Tallahassee, Florida 32310, USA
[2]National High Magnetic Field Laboratory, Tallahassee, Florida 32310, USA
[3]Department of Mechanical and Energy Engineering, Southern University of Science and Technology, Shenzhen 518055, China

[a]Electronic addresses: pbenhal@eng.famu.fsu.edu; david1.quashie@famu.edu; and cheanguk@sustech.edu.cn
[b]Author to whom correspondence should be addressed: jali@eng.famu.fsu.edu

ABSTRACT

Here we investigate the dynamic behavior of self-assembling achiral swimmers in viscous media. The response of magnetically actuated swimmers of two differing geometries is explored under various uniform rotational field frequencies and amplitudes. Kinematic characteristics obtained from tracked swimming motion, including speed, precession angle (wobbling angle), and re-orientation time (turning rate), are determined and reveal nonlinear relationships between the dynamic response of the achiral swimmers and fluid viscosity, which induces drag forces that reduce the speed of propulsion and turning rates. We also find distinct regimes of swimmer motion that are dependent on both fluid viscosity and swimmer geometry. Similar viscosity and geometric dependence is observed for turning rates of swimmers when undergoing rapid changes in field orientation. The characteristic results obtained for microswimmer motion in viscous fluids will contribute to the development of control strategies for propelling other simple swimmers with two or more planes of symmetry. Characterized propulsion kinematics will aid in the optimization of swimmer designs and actuation approaches, critical for future low Reynolds number applications.

Small scale swimmers are devices propelled by utilizing their surrounding low Reynolds number environments for propulsion. The concept and potential applications of micro/nanoscale machines were first proposed by Feynman[1] ("There's Plenty of Room at the Bottom") in the 1960s. Over the past two decades, tiny actuators in the form of swimmers have been actively investigated for their potential in a diverse range of fields, including drug delivery,[2–6] tissue engineering,[7–11] environmental remediation,[12–16] and microsurgery.[17,18]

In viscosity-dominated microenvironments, nonreciprocal (i.e., non-time symmetrical) motion is considered necessary to induce net forward propulsion.[19,20] The requirement of nonreciprocal propulsion was classically proposed by Purcell[21] in 1977 and is now known as the Scallop Theorem.[21,22] Over the past two decades, there have been a number of reports aimed at harnessing the nonreciprocal propulsion of various geometries to understand the dynamics of swimmer behavior in viscous fluids. For a successful future voyage in the human body, microswimmers need to be efficiently propelled in complex media which contain heterogeneous networks of biological polymers and possess a range of viscosities. To date, most microswimmers have used either chirality or flexibility for swimming across viscous barriers.[23–28] In addition to these, rigid achiral swimmers have also been demonstrated to achieve propulsion in time-varying rotational fields. Compared to chiral swimmers, achiral swimmers have structural simplicity and manufacturing scalability.[29–31] It has been shown that a minimal geometrical requirement for net propulsion in Stokes flows is geometric asymmetry rather than chirality or flexibility.[19,32] Cheang *et al.*[30,33] in 2014 were the first to propose the concept of achiral swimmers.[29,30] Additional work on achiral swimmers propelled using precessional magnetic fields has been presented[34] along with kinematic modeling of their motion. In 2017, Morozov *et al.*[35] proposed that chiral helical swimmers outperform achiral arc swimmers, as the step-out frequency of helical propellers is about twice that of arc-shaped swimmers.[35] However, it was also found that the achiral arc swimmer slightly outperformed the chiral helix in the range of frequencies where both propellers exhibit in-sync wobbling dynamics.[35] While theories concerning the dynamics of chiral helical magnetic propellers have been proposed and confirmed through experiments, propulsion of self-assembling achiral particles and objects with complex shapes are

currently not well understood.[35] In order to better understand the complex geometrical and dynamical movements of small scale swimmers, groups have used techniques including chemotaxis,[36–39] magnetic,[40–43] acoustic,[44–47] ultrasonic,[48,49] optical/thermal,[3,50] and electrostatic actuation[51–53] to propel devices. Among the various noncontact manipulation strategies, magnetically controlled actuation is relatively simple and can be applied to spherical geometries.[29,31,33,35] Magnetic fields have been used to propel a number of other particles with various other geometries, including erythrocytes,[54] magnetically actuated sperm cells,[55] rolling micromotors,[56] and DNA-based artificial bacterial flagella.[57]

Considering the future potential of magnetically actuated achiral objects for *in-vitro* and *in-vivo* systems, here we explore a translational and rotational motion of self-assembled achiral microswimmers toward understanding propulsion kinematics in viscous media. Using time-varying magnetic fields, we actuate achiral microswimmers consisting of 3 and 4 beads. We analyze the behavior of achiral microswimmers in water and methylcellulose (MC) solutions by applying rotating fields with frequencies ranging from 0 to 50 Hz and uniform field strengths up to 20 mT. In these rotating magnetic field ranges, step-out frequencies of achiral swimmers were determined. Swimmer controllability, propulsion characteristics, and kinematic quantities, such as speed, precession angle, and turning duration profiles, were also characterized.

Self-assembled achiral swimmers were prepared by adding a mixture of 4.35 μm diameter polystyrene beads coated with ferromagnetic iron oxide, functionalized with biotin (TM-40–10, Spherotech Inc.) or avidin (VM-40–10, Spherotech Inc.), into separate tubes containing either de-ionized (DI) water, 0.2%, 0.4%, or 0.6% (w/v) MC. The methylcellulose used (M0512, Sigma-Aldrich) has a molecular weight of 88 kDa and a dynamic viscosity of 4000 mPa · s at 2% (w/v) at 20 °C. These MC concentrations were chosen to match physiological viscosities of fluids found in the human body.[58] The MC solutions were prepared by initially dissolving 1.5 g of MC in 150 ml of DI water. Then, the mixture was magnetically stirred for ∼12 h at 1500 rpm at room temperature. The mixture was then filtered using a 110 μm pore size filter using suction filtration to remove large debris. The mixture was then double filtered using a 5 μm pore size filter. Finally, a filtered MC stock solution was obtained at a concentration of 1% (w/v). The stock solution was then diluted with DI water to obtain 0.6% (w/v), 0.4% (w/v), and 0.2% (w/v) MC. Mixtures of biotin-avidin beads added to DI and MC were vortexed at room temperature for 5 min before use [Fig. 1(a)]. Bulk shear rheology (MCR 302, Anton Paar) measurements were conducted to characterize the viscosities of the methylcellulose fluids used. Low shear rate measurements [Fig. S1(c)], representing the frequencies at which our experiments were conducted, reveal that all fluids used behave as Newtonian fluids.

The experimental setup used consists of a magnetic field generator (MagnebotiX MFG-100/100-i)[59,60] mounted on an inverted microscope. By applying time-varying signals, rotational actuation of magnetic particles was accomplished. Uniform magnetic fields produced using the MFG system have previously been reported by Schürle *et al.*[59] During experiments, self-assembled swimmers in a 10 μl sample volume were sealed in a polydimethylsiloxane (PDMS) chamber which was mounted on a standard borosilicate glass (25 × 75 mm^2) slide. A square cover glass (22 × 22 mm^2) was placed on top of the PDMS to form a sealed chamber. For analysis, it was essential

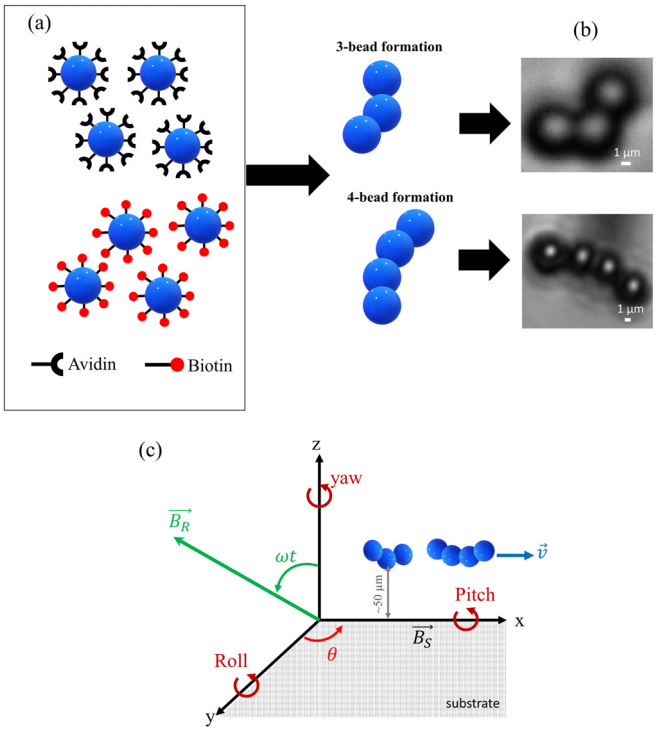

FIG. 1. (a) Microswimmer fabrication: avidin and biotin coated beads and mixed to form swimmers. (b) Bright-field images of self-assembled 3 and 4 bead structures. (c) Achiral microswimmer trajectory when subjected to magnetic fields.

that the observed swimmers were moving in bulk fluid rather than rolling along a boundary. In 0.4% and 0.6% w/v methylcellulose, swimmer settling was sufficiently slow as to not significantly affect the swimmer motion during experiments, whereas in 0.2% w/v methylcellulose, settling was much more rapid, and care was taken to perform experiments before swimmers reached near the glass substrate. Swimmers in DI water settled the fastest; however, this was somewhat mitigated by using a solution of saturated sodium chloride. If the swimmers are in contact with the substrate, rolling motion occurs, with displacement perpendicular to the rotation axis. In contrast, microswimmers actuated in a bulk fluid are propelled in the same direction as the rotation axis (pitch). Thus, to distinguish bulk swimming from surface motion while conducting the experiments, we recorded image sequences of swimming, 5–50 μm above the surface of the glass substrate to ensure only bulk swimming, free from surface boundary effects. Figure 1(c) shows a schematic of the microswimmers motion kinematics relative to the applied rotating magnetic field above the surface (not to scale). The microswimmer motion was visualized and captured using an inverted optical microscope system with a 40 × (1.5 × zoom) objective lens, and a CMOS camera was used for video recording of microswimmer motion at 30 (at 16-bit) frames per second (fps) with 1280 × 1024 pixels spatial resolution. The recorded microswimmer motion video is analyzed in Nikon Instrument Software (NIS v5.2). Each frame in the recorded video was tracked via the NIS analysis tracking algorithm. Data, including centroid position and speed vs time for each microswimmer, were determined.

The wobbling angles were obtained by the angle measurement tool in the NIS software.

Achiral beads subjected to rotating magnetic fields initially rotate and then translate between specific frequency ranges, following a helical trajectory.[29–31,61] If the swimmers are not flexible or chiral, propulsion can still be achieved as long as their structure satisfies the requirement of having a nonzero coupling tensor.[30,62] Based on a number of previously published theoretical and experimental results,[35,62,63] achiral swimmers of various geometries are capable of propulsion in uniform rotating magnetic fields because they have only one or two symmetric planes, which leads to a nonzero coupling tensor. Since the microswimmers are achiral, a helical trajectory can be maintained along any rotation axis, along x (pitch), y (roll), and z (yaw), as long as the swimmers are in a bulk fluid environment. With a reversal in field directions, the microswimmers trajectory can be changed left or right while swimming. The helical kinematic trajectory of each bead can be expressed as follows:[31]

$$x(t) = \vec{v}_x t, \tag{1}$$

$$y(t) = a\sin(\omega t + b) + c, \tag{2}$$

$$z(t) = a\cos(\omega t + b) + c, \tag{3}$$

where $\vec{v}_x$ is the velocity along the x-axis, t is time, ω is the rotation frequency, and a, b, c are constant parameters or coefficients of helical trajectory of each swimmer. These parameters can be determined by either experimental investigation or by numerical analysis.[29,61]

We experimentally determined and analyzed self-assembling 3 and 4 bead achiral beads swimming in various combinations of rotating magnetic field frequencies (1–50 Hz) and amplitudes (1–20 mT). We nondimensionalized the average speed (V) by dividing the speed by the swimmer characteristic length (l) and respective applied field frequencies (ω). The nondimensionalized plots shown in Fig. 2 provide useful information regarding the trends of the swimmers with respect to the applied field frequency. For example, as the concentration of the MC increases, the range of frequencies producing propulsion decreases. When comparing this decrease between the 3 and 4 bead achiral swimmers, the 4 bead swimmer's range is slightly larger which we attribute to the additional amount of magnetic material and change in rotational anisotropy. As reported by Morozov *et al.*,[35] the addition of a fourth bead brings the swimmer geometry, specifically the swimmer arc angle, closer to the optimal swimming geometry. The speed vs frequency peak trends in the supplementary material Fig. S2 show that 4 bead actuators swim 5%–10% faster than 3 beads in the four viscous fluids at the same field strength of 14 mT. In general, the microswimmers were found to follow three distinct swimming regimes or modes of motion (see supplementary material Fig. S2), similar to those reported previously.[29,64] These regimes are (1) near-symmetrical swimming (negligible propulsion), (2) nonsymmetrical swimming (translational propulsion), and (3) wiggling motion (no swimming). During symmetrical swimming, the beads only rotate along a symmetric axis in place and in phase with the applied rotation field, resulting in no net propulsion. Within the swimming regime, beads rotate in a nonsymmetrical manner, resulting in net forward thrust. Under the third regime of wiggling motion (observed after reaching a critical step-out frequency), the motion of the beads can be defined as asynchronous rotation without additional propulsion/motion. In the fluids used, a near-symmetrical swimming regime was only seen in DI water, and 0.2% MC at low frequencies for both 3 and 4 bead swimmers. In water, 3 bead swimmers were found to swim nonsymmetrically between 5 and 25 Hz, and after 25 Hz, the beads transition to wiggling with slowing asynchronous rotation, and at higher frequencies swimmers are not observed to completely rotate but rapidly oscillate. Compared to 3 beads, 4 bead achiral swimmers nonsymmetrical swimming was seen over a larger range of frequencies at the same field strength. Overall, the peak shifts show a trend in nonsymmetrical swimming. Similarly, we can see peaks in speeds shifting toward lower frequency regions with increasing MC concentration. These observed results can be interpreted as the resultant effects of increased fluid resistance with increasing polymer concentration, reducing the Brownian motion of the swimmers, and hindering wobbling motion.

In buffer solutions, the velocity of chrial and achiral microswimmers can be adjusted linearly with field rotation frequency; however, the presence of polymers is known to introduce nonlinearity into this relationship for chiral swimmers. As it is unknown if similar behavior is observed for achiral swimmers in polymer solutions, we applied constant frequency/field ratios to determine achiral propulsion kinematics in MC solutions and nondimensionalized their swimming speeds. Here nondimensionalization was performed by dividing the

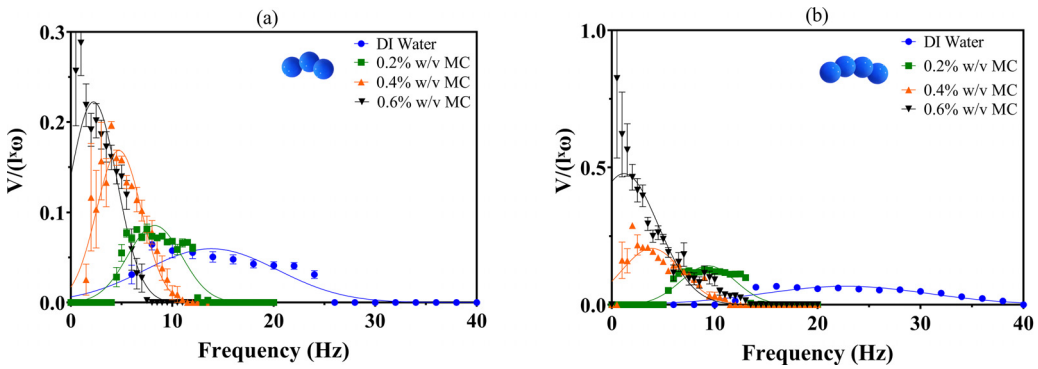

FIG. 2. Nondimensional average swimming speed (V) of ten different (N = 10) microswimmers with an increase in magnetic field frequency. The average speed is divided by the characteristic length (l) of swimmers and respective applied field frequencies, (a) 3 bead achiral swimmer in DI water and 0.2%, 0.4%, and 0.6% (w/v) MC. (b) 4 bead achiral swimmer in DI water and 0.2%, 0.4%, and 0.6% (w/v) MC. Lines indicate nonlinear Gaussian fit, and error bars indicate standard error from the mean speed.

swimmers' speed in DI water. In DI water and 0.2% MC, we observed approximately a linear relationship between speed vs frequency, at constant frequency/field ratio [see Figs. 3(b) and 3(c)]. However, at higher MC concentrations we observe increasingly nonlinear behavior between speed and frequency, which is more distinct for 4 bead swimmers. This again may be due to differences in rotational anisotropy mentioned previously.[35] Plots of speed vs frequency/field ratio as shown in Figs. S3(a), S3(c), S3(e), and S3(g) and nondimensionalized Figs. 3(b) and 3(c) provide means to modulate the velocity of microswimmers linearly with rotation frequency on the same rotation axis. The ratio plots can be used to apply magnetic fields on microswimmers of varying magnetic content to obtain specific swimming characteristics.[61] Apart from quantifying speed vs frequencies, we also measured the speed of the achiral 3 and 4 bead swimmers with respect to their precession or wobbling angle and frequency/field ratio [see Figs. S3(b), S3(d), S3(f), and S3(h) and nondimensionalized Figs. 3(d)

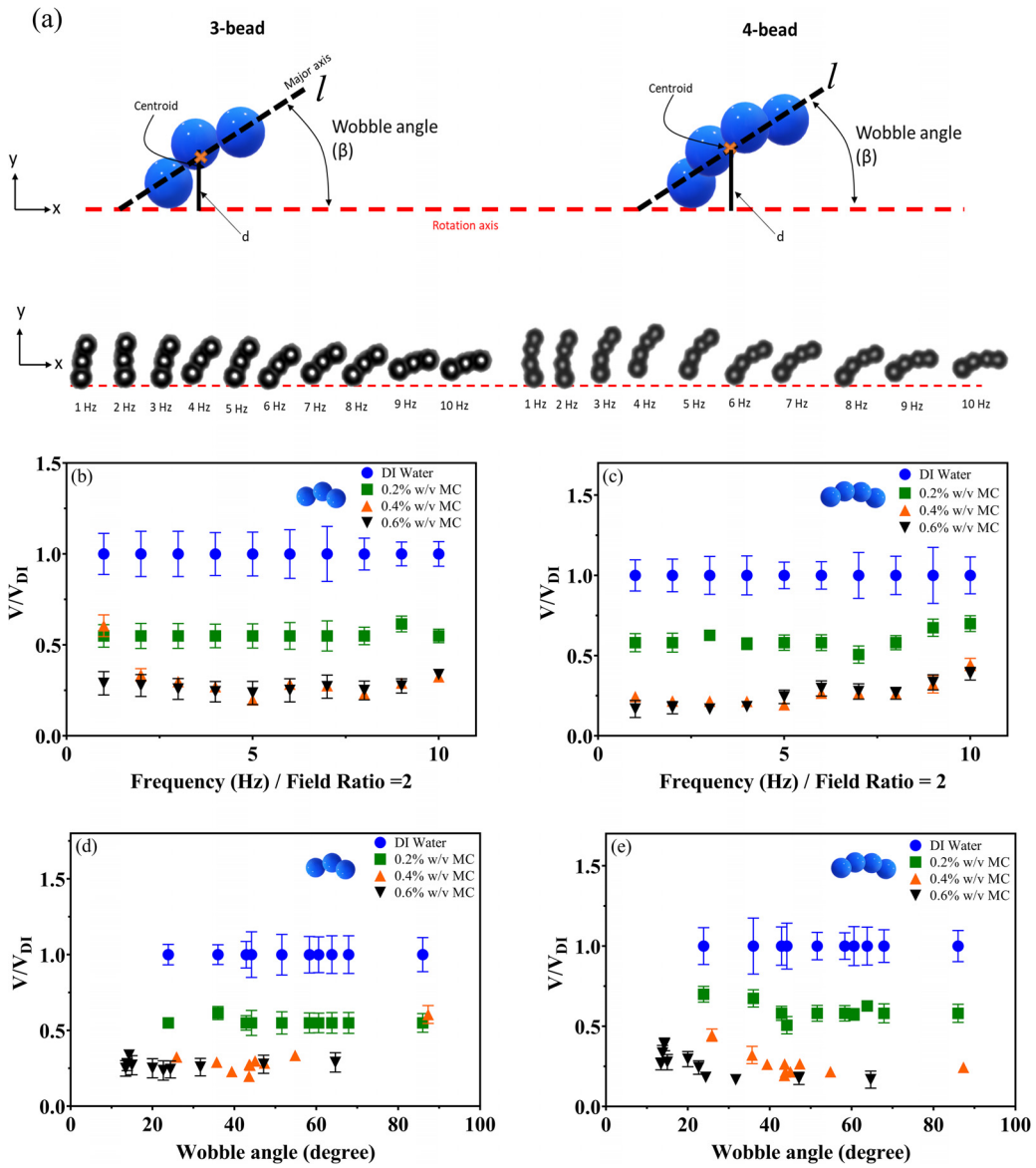

FIG. 3. Achiral bead speed vs frequency/amplitude ratio plots (N = 10 samples). (a) Sketch showing wobble angle measurements. (b) 3 bead swimmer nondimensionalized plots of speed vs frequency ratio in DI water, 0.2%, 0.4%, and 0.6% (w/v) MC. Speed is normalized using the speed in DI water. (c) 4 bead swimmer nondimensionalized plots of speed vs frequency ratio in DI water, 0.2%, 0.4%, and 0.6% (w/v) MC. Speed was normalized using the speed in DI water. (d) 3 bead swimmer nondimensionalized wobbling angle in DI water, 0.2%, 0.4%, and 0.6% (w/v) MC. (e) 4 bead swimmer nondimensionalized wobbling angle in DI water, 0.2%, 0.4%, and 0.6% (w/v) MC. Speed (V) was normalized using the speed in DI water (V_{DI}).

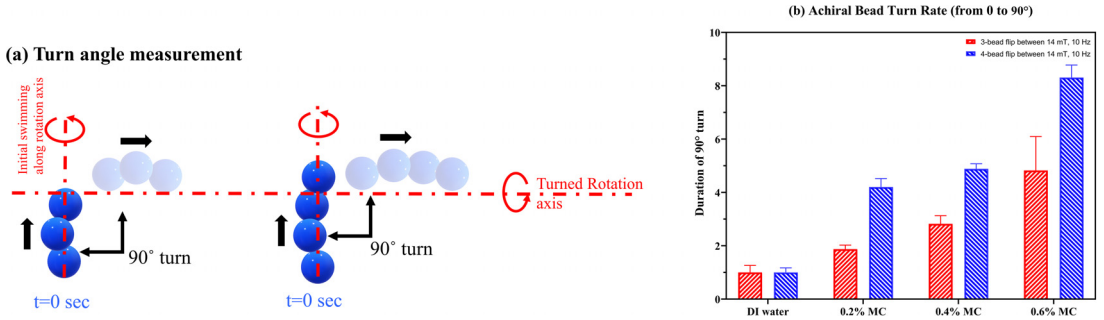

FIG. 4. Turning rate of achiral microswimmer. The swimmers are made to turn from 0 to 90° during swimming. (a) Sketch showing the turning rate measurement. (b) Duration of achiral microswimmer turns in MC solutions, normalized by turn duration in DI water.

and 3(e)]. The precession or wobbling angle is defined by the angle β between the rotation axis and the easy axis l of the microswimmers, as shown in Fig. 3(a). As wobble angle decreases, the swimming speed of microswimmers was found to increase in all fluids. When the achiral swimmers are in 0.2% w/v MC, we observed a near-linear increase in wobble angle with respect to decreasing speed. However, it was observed that increasingly more pronounced nonlinear decay (as speed decreases) coincides with increasing MC concentration (see Fig. S3). Wobble angle of swimmers, therefore, overall appears to decrease (with increasing speed) nonlinearly with viscous media. This trend is additional evidence that fluid viscosity plays a critical role in determining achiral microswimmer kinematics.

In addition to controlling their speed and precession angles, for practical applications where it is critical to efficiently guide swimmers to desired locations, it is necessary to understand the behavior and duration of achiral microswimmer's turning rate in response to changing magnetic fields. We, therefore, performed sharp (0–90°) turns for 3 and 4 beads during nonsymmetrical swimming, at swimmer's peak translational speeds. We measured the duration of turns in terms of their turn rate in DI water (Fig. 4). The duration of the turn for 3 bead and 4 bead achiral microswimmers in DI water was found to be in the range of 0.1–0.2 s to turn 90°. For both swimmer geometries, the duration of turn in 0.6% MC was 6%–8% slower than when in DI or 0.2% MC. This can be attributed to the drag forces influencing a slower turning rate. Similarly, in 0.2–0.4% MC, both achiral beads show a 3%–5% slower turn than when the beads are in DI. These turning rate measurements provided insight that in viscous media more power, magnetic field strength, and/or magnetic particle volume are necessary to quickly turn swimmers. Further, drag forces were found to be dominating over turn rate rather than the size of the swimmers. We determined that magnetic field strengths between 5 and 20 mT were suitable to turn both swimmers; however, here we only presented turn data at 14 mT, since the same trend follows if one applies different field magnitudes.

In conclusion, we have characterized and analyzed the speed, precession angle, and turning rate of achiral microswimmers in viscous fluids under rotating magnetic fields. The speed of 4 bead swimmers was found to be 5%–10% more than 3 bead swimmers. Peaks in overall transitional speed with respect to applied field frequency were observed to decrease with increasing methylcellulose concentration. Three swimming regimes were observed: near-symmetrical swimming, nonsymmetrical swimming, and wiggling motion or no swimming. Increasing viscosity resulted in overall motion profiles to narrow, from higher frequency ranges (in DI water: 0–50 Hz for 4 bead, and 0–25 Hz for 3 bead) to lower ranges (in 0.6% MC: 0–15 Hz for 4 bead and 0–10 Hz for 3 bead). Near-symmetrical swimming was only observed in low viscosity fluids, whereas similar initial near-symmetrical swimming behavior was not observed in higher viscosity fluids (0.4%–0.6% MC). Nonsymmetrical swimming regimes were present in all four fluids explored, and the size of this swimming regime was efficiently controlled with fluid viscosity modulation. After reaching step-out frequencies, the wiggling or no swimming regime was seen in all four viscous media, and the observed wiggling range was observed to widen with increasing fluid viscosity. We also determined that a nonlinear relationship existed between the viscosity of the media and the precession angle of achiral swimmers. In general, the speed of achiral swimmers, as with chiral swimmers, increases with a decreasing swimmer precession or wobbling angle. It is to be noted that the achiral swimmers reported in our article are reminiscent in size to a number of motile bacteria, such as *E. coli*; however, in our investigations with the self-assembled magnetic bead swimmers, we did not observe similar swimming enhancement that has been observed for *E. coli* in the MC fluids (see Table I in supplementary material).[65–67] We attribute the differences mainly due to lack of a thin rapidly rotating filament (flagellum) that is on the length scale of the polymer solution, which can induce lower local viscosities in the swimmer vicinity. Finally, it was observed that the turn rate of the achiral microswimmers monotonically increases with increasing viscosity. The observed kinematics of self-assembled 3 and 4 bead swimmers presented here serve as a first step in exploring the effects of polymer fluids on low Reynolds number achiral propulsion and kinematics, which will aid in the development of future achiral microswimmer applications and deployment strategies.

See the supplementary material for dimensional versions of Figs. 2 and 3, rheological measurements of dilute methylcellulose solutions, *E. coli* and achiral swimmer comparisons, and videos of magnetic actuation of swimmers in methylcellulose.

AUTHORS' CONTRIBUTIONS

P.B. and D.Q. contributed equally to this work.

This work was funded by the National Science Foundation (Nos. HDR-2000202 and CMMI-2000330) and support by the NSF FAMU CREST Center award (No. HDR-1735968). This work was also funded by the Science and Technology Innovation Committee Foundation of Shenzhen (No. JCYJ20180302174151692) and the Shenzhen municipal government (Peacock Plan, No. 20181119590C) awarded to U. Kei Cheang. All the work was performed at the National High Magnetic Field Laboratory, which is supported by National Science Foundation Cooperative Agreement Nos. DMR-1157490 and DMR-1644779 and the State of Florida.

DATA AVAILABILITY

The data supporting the findings of this investigation are available from the corresponding author upon reasonable request.

REFERENCES

[1]R. P. Feynman, California Inst. Technol. J. Eng. Sci. **4**(2), 22–23 (1959).
[2]B. W. Park, J. Zhuang, O. Yasa, and M. Sitti, ACS Nano **11**(9), 8910–8923 (2017).
[3]X. Peng, Z. Chen, P. S. Kollipara, Y. Liu, J. Fang, L. Lin, and Y. Zheng, Light: Sci. Appl. **9**(1), 141 (2020).
[4]H. Ceylan, I. C. Yasa, O. Yasa, A. F. Tabak, J. Giltinan, and M. Sitti, bioRxiv:379024 (2018).
[5]A. I. Bunea and R. Taboryski, Micromachines **11**(1048), 1048 (2020).
[6]A. R. Sprenger, V. A. Shaik, A. M. Ardekani, M. Lisicki, A. J. T. M. Mathijssen, F. Guzmán-Lastra, H. Löwen, A. M. Menzel, and A. Daddi-Moussa-Ider, Eur. Phys. J. E **43**(9), 58 (2020).
[7]T. Li, L. Li, W. Song, L. Wang, G. Shao, and G. Zhang, ECS J. Solid State Sci. Technol. **4**(10), S3016–S3019 (2015).
[8]D. Vilela, J. Parmar, Y. Zeng, Y. Zhao, and S. Sánchez, Nano Lett. **16**(4), 2860–2866 (2016).
[9]D. A. Uygun, B. Jurado-Sánchez, M. Uygun, and J. Wang, Environ. Sci.: Nano **3**(3), 559–566 (2016).
[10]J. Li, V. V. Singh, S. Sattayasamitsathit, J. Orozco, K. Kaufmann, R. Dong, W. Gao, B. Jurado-Sanchez, Y. Fedorak, and J. Wang, ACS Nano **8**(11), 11118–11125 (2014).
[11]F. Mushtaq, A. Asani, M. Hoop, X.-Z. Chen, D. Ahmed, B. J. Nelson, and S. Pané, Adv. Funct. Mater. **26**(38), 6995–7002 (2016).
[12]J. Parmar, D. Vilela, K. Villa, J. Wang, and S. Sánchez, J. Am. Chem. Soc. **140**(30), 9317–9331 (2018).
[13]M. Safdar, J. Simmchen, and J. Jänis, Environ. Sci. **4**(8), 1602–1616 (2017).
[14]W. Gao and J. Wang, ACS Nano **8**(4), 3170–3180 (2014).
[15]M. Zarei and M. Zarei, Small **14**(30), 1800912 (2018).
[16]C. Richard, J. Simmchen, and A. Eychmüller, Z. Phys. Chem. **232**(5–6), 747–757 (2018).
[17]J. Vyskočil, C. C. Mayorga-Martinez, E. Jablonská, F. Novotný, T. Ruml, and M. Pumera, ACS Nano **14**(7), 8247–8256 (2020).
[18]K. Harada, K. Masamune, I. Sakuma, N. Yahagi, T. Dohi, H. Iseki, and K. Takakura, in *Human Friendly Mechatronics*, edited by E. Arai, T. Arai, and M. Takano (Elsevier Science, Amsterdam, 2001), pp. 75–80.
[19]T. Qiu, T.-C. Lee, A. G. Mark, K. I. Morozov, R. Münster, O. Mierka, S. Turek, A. M. Leshansky, and P. Fischer, Nat. Commun. **5**(1), 5119 (2014).
[20]O. Yasuda, M. Kuroda, and S. Komura, Phys. Fluids **32**(9), 093102 (2020).
[21]E. M. Purcell, Am. J. Phys. **45**(1), 3–11 (1977).
[22]E. Lauga, Soft Matter **7**(7), 3060–3065 (2011).
[23]M. Mijalkov and G. Volpe, Soft Matter **9**(28), 6376–6381 (2013).
[24]B.-Q. Ai, Y.-F. He, and W.-R. Zhong, Soft Matter **11**(19), 3852–3859 (2015).
[25]R. P. Doherty, T. Varkevisser, M. Teunisse, J. Hoecht, S. Ketzetzi, S. Ouhajji, and D. J. Kraft, Soft Matter **16**(46), 10463–10469 (2020).
[26]G. Jing, A. Zöttl, É. Clément, and A. Lindner, Sci. Adv. **6**(28), eabb2012 (2020).
[27]B. Zhang, A. Sokolov, and A. Snezhko, Nat. Commun. **11**(1), 4401 (2020).
[28]A. C. H. Tsang, E. Demir, Y. Ding, and O. S. Pak, Adv. Intell. Syst. **2**(8), 1900137 (2020).
[29]U. K. Cheang, H. Kim, D. Milutinović, J. Choi, and M. J. Kim, J. Bionic Eng. **14**(2), 245–259 (2017).
[30]U. K. Cheang, F. Meshkati, D. Kim, M. J. Kim, and H. C. Fu, Phys. Rev. E **90**(3), 033007 (2014).
[31]L. Tan, J. Ali, U. K. Cheang, X. Shi, D. Kim, and M. J. Kim, Micromachines **10**(12), 865 (2019).
[32]J. Sachs, K. I. Morozov, O. Kenneth, T. Qiu, N. Segreto, P. Fischer, and A. M. Leshansky, Phys. Rev. E **98**(6), 063105 (2018).
[33]U. K. Cheang, M. Dejan, J. Choi, and M. Kim, in Presented at the ASME 2014 Dynamic Systems and Control Conference (2014).
[34]U. K. Cheang and M. J. Kim, J. Nanopart. Res. **17**(3), 145 (2015).
[35]K. I. Morozov, Y. Mirzae, O. Kenneth, and A. M. Leshansky, Phys. Rev. Fluids **2**(4), 044202 (2017).
[36]C. Jin, C. Krüger, and C. C. Maass, Proc. Natl. Acad. Sci. U. S. A. **114**(20), 5089–5094 (2017).
[37]E. Lauga, W. R. DiLuzio, G. M. Whitesides, and H. A. Stone, Biophys. J. **90**(2), 400–412 (2006).
[38]B. M. Friedrich and F. Jülicher, Proc. Natl. Acad. Sci. U. S. A. **104**(33), 13256–13261 (2007).
[39]O. Schauer, B. Mostaghaci, R. Colin, D. Hürtgen, D. Kraus, M. Sitti, and V. Sourjik, Sci. Rep. **8**(1), 9801–9801 (2018).
[40]R. S. M. Rikken, R. J. M. Nolte, J. C. Maan, J. C. M. van Hest, D. A. Wilson, and P. C. M. Christianen, Soft Matter **10**(9), 1295–1308 (2014).
[41]J. Giltinan, P. Katsamba, W. Wang, E. Lauga, and M. Sitti, Appl. Phys. Lett. **116**(13), 134101 (2020).
[42]J. García-Torres, C. Calero, F. Sagués, I. Pagonabarraga, and P. Tierno, Nat. Commun. **9**(1), 1663 (2018).
[43]W. Gao, X. Feng, A. Pei, C. R. Kane, R. Tam, C. Hennessy, and J. Wang, Nano Lett. **14**(1), 305–310 (2014).
[44]K. H. Lam, Y. Li, Y. Li, H. G. Lim, Q. Zhou, and K. K. Shung, Sci. Rep. **6**, 37554–37554 (2016)..
[45]M. A. Ghanem, A. D. Maxwell, Y.-N. Wang, B. W. Cunitz, V. A. Khokhlova, O. A. Sapozhnikov, and M. R. Bailey, Proc. Natl. Acad. Sci. U. S. A. **117**(29), 16848–16855 (2020).
[46]C. R. P. Courtney, C. E. M. Demore, H. Wu, A. Grinenko, P. D. Wilcox, S. Cochran, and B. W. Drinkwater, Appl. Phys. Lett. **104**(15), 154103 (2014).
[47]L. Ren, N. Nama, J. M. McNeill, F. Soto, Z. Yan, W. Liu, W. Wang, J. Wang, and T. E. Mallouk, Sci. Adv. **5**(10), eaax3084 (2019)..
[48]K. H. Lam, H.-S. Hsu, Y. Li, C. Lee, A. Lin, Q. Zhou, E. S. Kim, and K. K. Shung, Biotechnol. Bioeng. **110**(3), 881–886 (2013).
[49]X. Chen, X. Qian, K.-H. Lam, C. T. Chiu, R. Chen, Z. Chen, K. K. Shung, P. Yu, and Q. Zhou, Adv. Funct. Mater. **29**(32), 1902912 (2019).
[50]F. Lancia, T. Yamamoto, A. Ryabchun, T. Yamaguchi, M. Sano, and N. Katsonis, Nat. Commun. **10**(1), 5238 (2019).
[51]X. Zhan, J. Wang, Z. Xiong, X. Zhang, Y. Zhou, J. Zheng, J. Chen, S.-P. Feng, and J. Tang, Nat. Commun. **10**(1), 3921 (2019).
[52]J. Roche, S. Carrara, J. Sanchez, J. Lannelongue, G. Loget, L. Bouffier, P. Fischer, and A. Kuhn, Sci. Rep. **4**(1), 6705 (2015).
[53]G. Hwang, R. Braive, L. Couraud, A. Cavanna, O. Abdelkarim, I. Robert-Philip, A. Beveratos, I. Sagnes, S. Haliyo, and S. Régnier, Int. J. Rob. Res. **30**(7), 806–819 (2011).
[54]R. Dreyfus, J. Baudry, M. L. Roper, M. Fermigier, H. A. Stone, and J. Bibette, Nature **437**(7060), 862–865 (2005).
[55]I. S. M. Khalil, V. Magdanz, J. Simmchen, A. Klingner, and S. Misra, Appl. Phys. Lett. **116**(6), 063702 (2020).
[56]M. Vilfan, N. Osterman, and A. Vilfan, Soft Matter **14**(17), 3415–3422 (2018).
[57]A. M. Maier, C. Weig, P. Oswald, E. Frey, P. Fischer, and T. Liedl, Nano Lett. **16**(2), 906–910 (2016).
[58]B. J. Nelson and K. E. Peyer, ACS Nano **8**(9), 8718–8724 (2014).
[59]S. Schuerle, S. Erni, M. Flink, B. E. Kratochvil, and B. J. Nelson, IEEE Trans. Magn. **49**(1), 321–330 (2013).
[60]S. Schuerle, I. A. Vizcarra, J. Moeller, M. S. Sakar, B. Özkale, A. M. Lindo, F. Mushtaq, I. Schoen, S. Pané, V. Vogel, and B. J. Nelson, Sci. Rob. **2**(2), eaah6094 (2017).

[61]U. K. Cheang and M. J. Kim, Appl. Phys. Lett. **109**(3), 034101 (2016).
[62]S. Tottori and B. J. Nelson, Small **14**(24), e1800722 (2018).
[63]F. Meshkati and H. C. Fu, Phys. Rev. E **90**(6), 063006 (2014).
[64]U. K. Cheang, K. Lee, A. A. Julius, and M. J. Kim, Appl. Phys. Lett. **105**(8), 083705 (2014).
[65]A. E. Patteson, A. Gopinath, M. Goulian, and P. E. Arratia, Sci. Rep. **5**(1), 15761 (2015)..
[66]W. R. Schneider and R. N. Doetsch, J. Bacteriol. **117**(2), 696–701 (1974).
[67]L. Turner, L. Ping, M. Neubauer, and H. C. Berg, Biophys. J. **111**(3), 630–639 (2016).